

Twentieth-Century Sea Surface Temperature Trends

Mark A. Cane *et al.*

Science **275**, 957 (1997);

DOI: 10.1126/science.275.5302.957

This copy is for your personal, non-commercial use only.

If you wish to distribute this article to others, you can order high-quality copies for your colleagues, clients, or customers by [clicking here](#).

Permission to republish or repurpose articles or portions of articles can be obtained by following the guidelines [here](#).

The following resources related to this article are available online at www.sciencemag.org (this information is current as of May 27, 2014):

Updated information and services, including high-resolution figures, can be found in the online version of this article at:

<http://www.sciencemag.org/content/275/5302/957.full.html>

This article **cites 19 articles**, 2 of which can be accessed free:

<http://www.sciencemag.org/content/275/5302/957.full.html#ref-list-1>

This article has been **cited by 9 articles** hosted by HighWire Press; see:

<http://www.sciencemag.org/content/275/5302/957.full.html#related-urls>

This article appears in the following **subject collections**:

Atmospheric Science

<http://www.sciencemag.org/cgi/collection/atmos>

- angstroms. Therefore, the magnitude of ν can be determined as precisely as needed by choosing a sufficiently large time interval ($t_2 - t_1$) between the corresponding measurements of z .
9. Analysis of structures means that the structures were animated by the use of the Xmol program. Visual inspection of snapshots (similar to those available to online subscribers at <http://www.sciencemag.org>) allowed me to distinguish between solid and liquid structures. This procedure was successfully applied in the determination of the melting curve of MgO [A. Belonoshko and L. S. Dubrovinsky, *Am. Mineral.* **81**, 303 (1996)], and in the case of a monatomic substance it is even more reliable.
 10. V. Y. Klimenko and A. N. Dremnin, in *Detonatsiya*, O. N. Breusov, Ed. (Akademii Nauk, Moscow, 1978), p. 79.
 11. R. D. Dick, R. H. Warnes, J. Skalyo, *J. Chem. Phys.* **53**, 1648 (1970).
 12. J. M. Brown and R. G. McQueen, *J. Geophys. Res.* **91**, 7485 (1986).
 13. R. Boehler suggested in his talk at the Structure of Earth Deep Interior VI Symposium (July 1996) that Brown and McQueen (12) observed only one discontinuity and that this discontinuity is related to melting. According to the results of my study, it is likely that indeed two discontinuities were observed.
 14. I am grateful to O. L. Anderson, M. Brown, and F. Seifert for helpful discussions. Comments by two anonymous reviewers were useful. Simulations were done with the use of the IBM SP2 in the Parallel Computer Center in Stockholm. The research was supported by Swedish Natural Science Council (Naturvetenskapliga Forskningsrådet) grant G-Gu 06901-301.

25 September 1996; accepted 30 December 1996

Twentieth-Century Sea Surface Temperature Trends

Mark A. Cane,* Amy C. Clement, Alexey Kaplan, Yochanan Kushnir, Dmitri Pozdnyakov, Richard Seager, Stephen E. Zebiak, Ragu Murtugudde

An analysis of historical sea surface temperatures provides evidence for global warming since 1900, in line with land-based analyses of global temperature trends, and also shows that over the same period, the eastern equatorial Pacific cooled and the zonal sea surface temperature gradient strengthened. Recent theoretical studies have predicted such a pattern as a response of the coupled ocean-atmosphere system to an exogenous heating of the tropical atmosphere. This pattern, however, is not reproduced by the complex ocean-atmosphere circulation models currently used to simulate the climatic response to increased greenhouse gases. Its presence is likely to lessen the mean 20th-century global temperature change in model simulations.

Amidst the often contentious debate on global warming, there are areas of general consensus. There is agreement that Earth's surface temperature has increased over the last 100 years by between $\sim 0.3^\circ$ and 0.6°C (1). There is, however, disagreement as to the causes of this temperature increase. It may be a response to anthropogenic forcing, a part of the climate system's innate natural variability, or a combination of the two. There is also general consensus that the radiative effect of increased atmospheric concentrations of greenhouse gases will cause Earth's temperature to rise. The direct warming effect of these gases is rather small, but there is a potential for amplification by positive feedbacks within the climate system. Understanding of these mechanisms is incomplete, and the strength of the amplification is uncertain, as evidenced

by the fact that, when loaded with twice the modern concentration of atmospheric CO_2 , state-of-the-art climate models give mean global changes varying from 1.5° to 4.5°C (1).

Until quite recently, simulations of the climatic response to increasing concentrations of greenhouse gases gave temperature changes that exceeded the observed increase by about a factor of 2 (1, 2). It was then suggested that the discrepancy might result from the neglect of the cooling effect of sulfate aerosols (3). Inclusion of this effect brought simulations into better agreement with observations (1, 2). Unfortunately, the radiative effects of aerosols are poorly understood. It is quite possible that the influence of the values currently used in simulations is considerably larger than the true influence (4) and is substituting for natural moderating mechanisms that are absent or underrepresented in present models.

Here we point out a pattern in the changes of sea surface temperature (SST) over the course of the 20th century—an increase in the zonal gradient across the equatorial Pacific—that has been missed in simulations performed with comprehensive climate models [general circulation models

(GCMs)]. Recent theoretical studies (5–8) have predicted this pattern as a response to exogenous heating of the tropical atmosphere. If the theory is correct, it would provide evidence that the coupled atmosphere-ocean dynamics are delaying, and possibly regulating, global warming. The absence of this mechanism in the GCM simulations may account in part for the discrepancy between the observed and modeled global mean temperature rise.

The theoretical ideas we invoke (5–8) follow the line of argument first proposed by Bjerknes (9), which forms the foundation of our present understanding of the El Niño–Southern Oscillation (ENSO) phenomenon (10). Suppose a uniform external heating is imposed on the tropical Pacific. The SST will tend to rise, leading to increased evaporative cooling until a new, warmer equilibrium is reached. This change would be the only response in the absence of a decisive contribution from ocean dynamics. In the eastern equatorial region, however, vigorous upwelling brings up cold waters from below, counteracting the warming tendency. Thus, initially, the SST increases more in the west than in the east, enhancing the temperature gradient along the equator. The atmosphere responds with increasing trade winds, which in turn will increase the upwelling rate and the thermocline (11) tilt, cooling the surface waters in the east and further enhancing the temperature contrast. As a consequence of this dynamical feedback, the mean temperature will increase less than it would with the purely thermodynamic response.

To test the mechanism, we imposed a uniform forcing on a simplified model of the ocean-atmosphere system in the tropical Pacific, the Lamont model used to forecast El Niño (12). The forcing was chosen so that in the absence of ocean dynamics, SST would increase by 1°C everywhere. In the model's mean annual response (Fig. 1), not only does the eastern equatorial Pacific cool, consistent with the mechanism described above, but the dynamics of the coupled ocean atmosphere system spreads the influence of the upwelled waters throughout the tropical Pacific, such that the mean increase in temperature is only 0.5°C .

A number of objections to this theory and model demonstration may be raised. The theory relies on colder upwelled waters balancing some of the imposed heat input, but the simple ocean model used specifies a fixed thermocline temperature. In reality, the waters of the equatorial thermocline originate at the surface at higher latitudes. If these source waters were to warm up, then equatorial thermocline temperatures would eventually increase; the cooling effect would then be reduced on a time scale set by the renewal time for the equatorial thermocline. Some recent

M. A. Cane, A. C. Clement, A. Kaplan, Y. Kushnir, D. Pozdnyakov, R. Seager, S. E. Zebiak, Lamont-Doherty Earth Observatory, Palisades, NY 10964–8000, USA. R. Murtugudde, Universities Space Research Association, Laboratory for Hydrospheric Processes, NASA Goddard Space Flight Center, Greenbelt, MD 20771, USA.

*To whom correspondence should be addressed.

studies place the origin of equatorial thermocline waters in the subtropics, which suggests a renewal time of a few decades (13). However, there is persuasive evidence that the waters of the high-latitude Southern Hemisphere are a significant source (14), implying a longer renewal time.

Because the origin of equatorial thermocline waters and this renewal time are not well determined by observations, we turn to numerical simulation. An ocean GCM was run with a realistic SST-dependent heat flux formulation to which a uniform heating of 10 W m^{-2} was added (15). In contrast to the previous model (Fig. 1), the wind stress was fixed at climatological values. Even so, while the eastern equatorial Pacific warmed slightly, the western Pacific warmed more (Fig. 2). This increase in zonal gradient persisted over the duration of the run; it is thus not a transient effect. Even without the feedback to the winds, the overall warming from 30°N to 30°S was reduced to two-thirds of that in the absence of ocean dynamics (15).

The smallness of the eastern equatorial thermocline warming ($\sim 0.3^\circ\text{C}$) is due in part to the very strong mixing in the equatorial thermocline: waters flowing in from the subtropics are strongly diluted, including waters in the lower thermocline originating at high southern latitudes (14). Even apart from the equatorial zone, these flows are at depths too shallow not to be affected by mixing. These "leaks" in the subtropical to equatorial pipeline delay the adjustment of equatorial thermocline temperatures. Moreover, the amplitude of the adjustment is limited by the SST changes at the source latitudes. These changes are smaller than those in the tropics because stronger winds allow the latent heat fluxes to balance the imposed heating with smaller SST increases. By moving heat poleward, the ocean redistributes it to regions where it can more easily be lost to the atmosphere and ultimately to space. The global consequence is a reduction in the mean warming. For the equatorial ocean, it means that the thermocline warming is too small to overcome the cooling effect of the coupled dynamics.

Another objection to the above argument is that its prediction is in conflict with doubled CO_2 simulations performed with complex coupled GCMs, in which the eastern equatorial Pacific was found to warm more than the west (16, 17). The GCM results

were attributed to the lower mean SSTs in the east, which, in view of the Clausius-Clapeyron relation, require larger temperature changes to generate the same evaporative cooling as in the west (16). This effect is absent in the Lamont model but is present in the ocean GCM simulation (15) described above. In the latter simulation, these local thermodynamic effects are overwhelmed by equatorial upwelling (18).

We believe that the discrepancy between the results presented here and the coupled GCMs is explained by the difference in the strength of the dynamic coupling between the equatorial ocean and atmosphere (19). If the coupling is strong, then the Bjerknes feedback operates (5), resulting in the stronger gradient of Fig. 1. If the coupling is weak, then the thermodynamic equilibrium solution will hold, as with the low-resolution coupled GCMs used in greenhouse warming simulations (1, 16–18). That the interannual variability of these models is weaker than the observed ENSO cycle and has different patterns (20) supports the inference that the effective coupling strength of these models is weaker than in nature.

The most likely reason is that in global warming simulations, the ocean components of coupled GCMs are run at resolutions too coarse to resolve the equatorial oceans (16). Consequently, vertical velocities at the equator are too weak and the equatorial thermocline is too diffuse; both effects reduce the amplitude of vertical heat fluxes in response to wind changes. In addition, many atmospheric GCMs produce overly weak surface winds in response to SST gradients.

In order to find out which effects dominate in the real system, we analyzed observational Pacific SST data to determine whether the equatorial Pacific SST gradient has strengthened or weakened in the past century, a period in which anthropogenic greenhouse gases are known to have increased. We rely on a new analysis (21); both statistical theory and empirical example indicate that it provides the best estimate to date of monthly mean global SST anomalies. A least squares linear fit to the trend from 1900 to 1991 (22) was performed at each point of the analysis (Fig. 3A). There is a warming almost everywhere, the notable exceptions being much of the North Pacific, a region south of Greenland, and the eastern equatorial Pacific. All of these cooling

areas and most of the neutral (warming $< 0.1^\circ\text{C}$) areas are significantly different at the 95% level from the global mean warming trend of 0.4°C per century. Although the match is far from perfect, the tropical Pacific part of this pattern is more similar to the Lamont model result in Fig. 1 (23) than to the enhanced eastern warming of the GCM experiments. The tropical Pacific cooling has not been noted previously. It is centered in a region with very few observations, and our analysis procedure (21) fills holes by making statistically optimal use of the covariance structure of the global SST field. Compared with earlier procedures used to create SST products, it is a more effective and unbiased way to compensate for secular changes in sampling.

It is notable that the eastern equatorial Pacific shows a cooling trend despite the strong and frequent El Niño events in the period after 1975. According to one point of view, the unusual period after 1975 is a consequence of the century-long warming trend (24). Another point of view is that the frequent El Niño events at the end of the period may be a chance occurrence due to natural variation (25) and should be excluded in reckoning trends. Doing so results in an even stronger cooling in the eastern Pacific (Fig. 3B), enhancing the resemblance to Fig. 1.

For our argument, the most salient feature of these trend estimates is the enhanced zonal gradient in the equatorial Pacific (26). To see if it is an artifact of the analysis procedure, we computed the change in zonal SST gradient from two other data compilations: GOSTA (27), which corrects for systematic measurement errors in bucket temperatures, and COADS (28), which does

Fig. 1. Annual mean SST anomaly (in degrees Celsius) generated by the Lamont intermediate coupled ocean-atmosphere model (12) when forced by an imposed uniform heating. [Adapted from (7)]

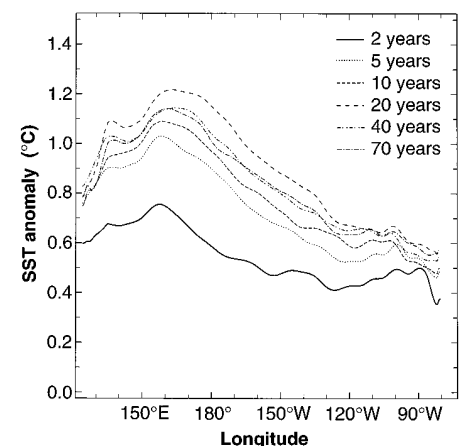
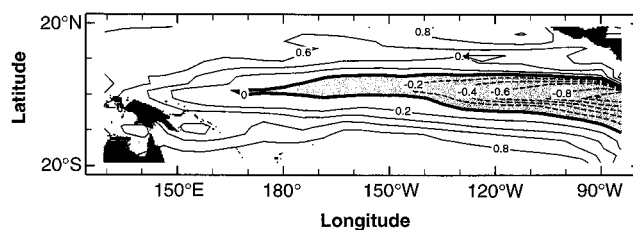


Fig. 2. Results from an ocean GCM simulation (15) with fixed winds and a realistic surface heat flux formulation to which a uniform heating of 10 W m^{-2} has been added. Changes in SST gradient along the equator from the initial state is shown for years 2, 5, 10, 20, 40, and 70. Most of the adjustment takes place in the first 2 years, and the steady state is closely approached by year 40.

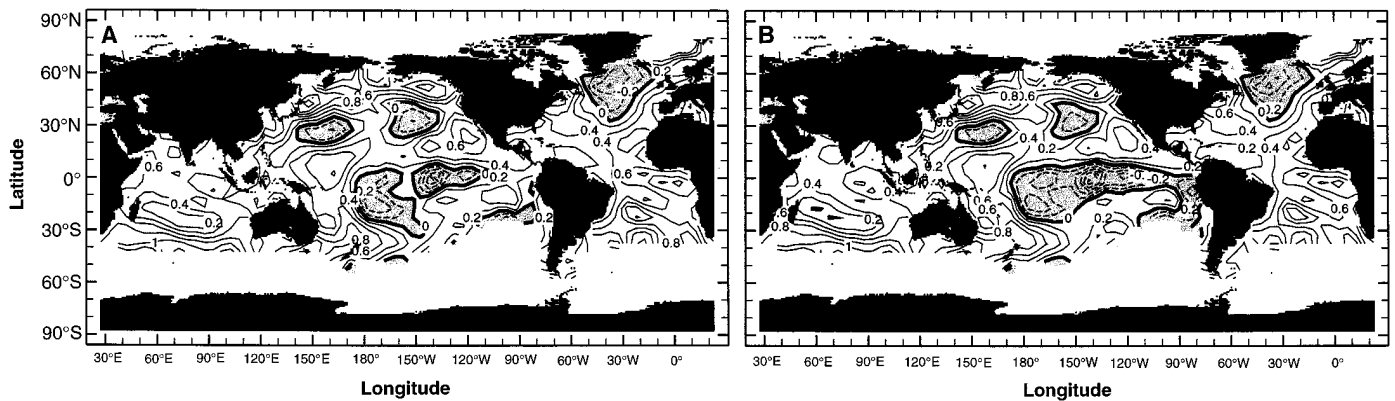


Fig. 3. (A) The trend in monthly mean SST anomalies for 1900 to 1991 in degrees Celsius per century. The SST fields are from an optimal smoother analysis (27). **(B)** As in (A), except that the influence of the large number of ENSO warm events at the end of the record was screened out before the

trend was calculated. This was done by removing the ENSO mode, defined as the leading empirical orthogonal function of the variability in the 2- to 7-year band. The projection of this pattern onto the data was subtracted from the record, and the trend in the remainder was computed.

not. As an index of zonal gradient, we used the difference between climatically important regions in the western (WP) and eastern (NINO3.4) equatorial Pacific. Although trends in the three data sets differ strongly within each region (Fig. 4), the trend in the gradient WP-NINO3.4 is more consistent. All three data sets show a strengthened gradient over the 20th century. In degrees Celsius per century with 95% confidence limits, the trend in the gradient is $+0.66 \pm 0.14$ for our analysis, $+0.11 \pm 0.15$ for GOSTA, and $+0.28 \pm 0.14$ for COADS (29). All three versions of the SST data support the predictions for strong atmospheric coupling (5-8) over the enhanced eastern warming of the greenhouse models (16-18). In addition, the

most relevant previous study (8), which included an analysis of trends since 1949, found an enhanced SST gradient as well as strengthened trade winds in both an atmospheric GCM and observational data.

Equatorial Pacific SST variations have a substantial impact on the global atmospheric circulation (30). The NINO3.4 region is thought to be the area of the tropical Pacific where SST anomalies have the strongest influence on the global atmosphere. Although we do not know how an atmospheric GCM would respond to the equatorial portion of the SST anomaly patterns of Fig. 3, the evidence suggests that atmospheric dynamics and thermodynamics would amplify the coupled negative feedback of the equa-

torial Pacific. First, the patterns have the general features of an ENSO cold event (La Niña), which is accompanied by a reduction of mean global atmospheric temperatures. Second, a recent report (31) examines the climate change associated with doubled atmospheric CO₂ as simulated by an atmospheric GCM coupled to an ocean mixed layer. In one experiment, the SST was computed everywhere, and in another, the SST was held artificially fixed in the eastern equatorial Pacific. The global surface air temperature change was 22% less in the second experiment.

A scenario consistent with data and theory is that the pattern of 20th-century SST warming combined with eastern equatorial Pacific cooling is a consequence of anthropogenic greenhouse gases. Dynamical coupling between the atmosphere and the tropical Pacific is delaying and regulating global warming. State-of-the-art models, which do not simulate this feedback fully, reproduce the observed temperature rise only if they compensate by assuming a very high value for the poorly known radiative effect of sulfate aerosols. The long-term consequences of the two processes, one an internal feedback and the other a temporary radiative forcing, would be quite different. It is thus important to determine how each contributes to the observed 20th-century temperature rise. Although equatorial Pacific ocean dynamics may delay and reduce global warming, the associated SST changes in the tropical Pacific would engender changes in regional climate and climate variability over much of the Earth that would be likely to have substantial social and economic consequences.

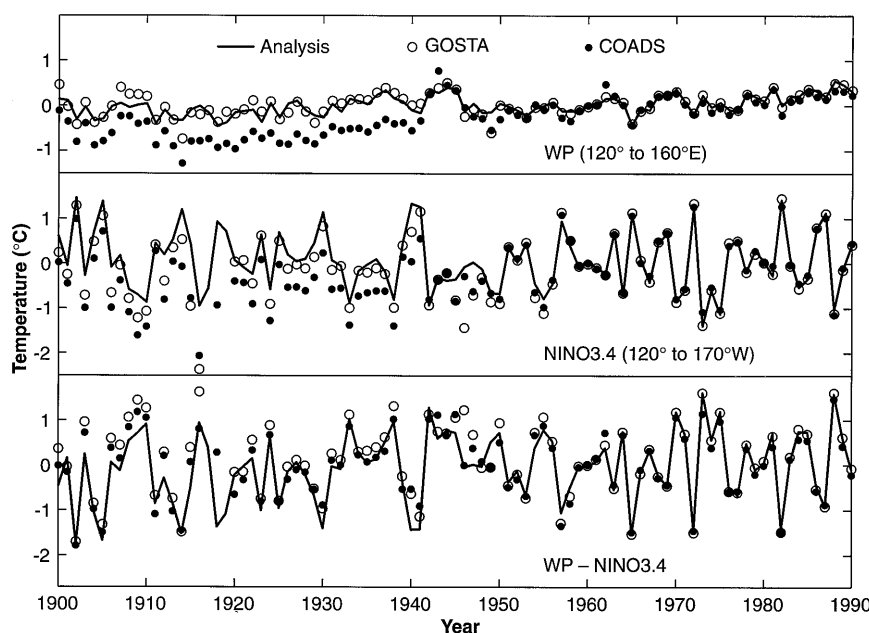


Fig. 4. Time series of (top) the average SST anomaly in the WP region (120° to 160°E, 5°N to 5°S), (middle) the average SST anomaly in the NINO3.4 region (120° to 170°W, 5°N to 5°S), and (bottom) the difference, a measure of the anomalous zonal SST gradient. Data from (solid curve) optimal smoother analysis (27), (open circles) GOSTA (27), and (closed circles) COADS (28).

REFERENCES AND NOTES

1. J. T. Houghton et al., Eds., *Climate Change 1995—The Science of Climate Change* (Cambridge Univ. Press, Cambridge, 1995).

2. J. F. B. Mitchell, T. C. Johns, J. M. Gregory, S. F. B. Tett, *Nature* **376**, 501 (1995).

3. R. J. Charlson *et al.*, *Science* **255**, 423 (1992).

4. J. T. Kiehl and B. P. Briegleb [*ibid.* **260**, 311 (1993)] and J. Hansen, M. Sato, and R. Ruedy [*Atmos. Res.* **37**, 175 (1995)] demonstrated that the direct radiative influence of sulfate aerosols is far too small to correct the simulations; it would have to be indirect, through their ability to alter cloud properties. The amplitude of the latter is highly speculative; compare (1) and A. Jones, L. Roberts, A. Slingo, *Nature* **370**, 450 (1994). Hansen, Sato, and Ruedy (in preparation) argue that the direct effect of the aerosols may be entirely canceled by a semidirect effect in which heating due to aerosol absorption reduces low cloud cover. Some inconsistencies of the aerosol cooling hypothesis with the observed spatial and temporal patterns of temperature change have been pointed out by T. R. Karl, R. W. Knight, G. Kukla, and J. Gavin [in *Aerosol Forcing of Climate*, R. J. Charlson and J. Heintzenberg, Eds. (Wiley, Chichester, UK, 1995), pp. 363–382].

5. D.-Z. Sun and Z. Liu, *Science* **272**, 1148 (1996).

6. J. D. Neelin and H. A. Dijkstra, *J. Clim.* **8**, 1325 (1995); H. A. Dijkstra and J. D. Neelin, *ibid.*, p. 1343.

7. A. C. Clement, R. Seager, M. A. Cane, S. E. Zebiak, *ibid.* **9**, 2190 (1996).

8. M. Latif, R. Kleeman, C. Eckert, in preparation.

9. J. Bjerknes, *Mon. Weather Rev.* **97**, 163 (1969).

10. M. A. Cane, in *Teleconnections Linking Worldwide Climate Anomalies*, M. Glantz, R. W. Katz, N. Nicholls, Eds. (Cambridge Univ. Press, Cambridge, 1991), pp. 345–369.

11. The thermocline is a region of sharp temperature change separating the warm surface layers from the cold abyssal waters.

12. S. E. Zebiak and M. A. Cane, *Mon. Weather Rev.* **115**, 2262 (1987). Details of the calculations used to produce Fig. 1 are described in (7). The model domain is 29°S to 29°N, 124°E to 80°W.

13. J. McCreary and P. Lu, *J. Phys. Oceanogr.* **24**, 466 (1994); Z. Liu, S. G. H. Philander, R. Pacanowski, *ibid.*, p. 1606.

14. J. R. Toggweiler, K. Dixon, W. S. Broecker, *J. Geophys. Res.* **96**, 20467 (1991).

15. R. Seager and R. Murtugudde, *J. Clim.*, in press.

16. T. R. Knutson and S. Manabe, *ibid.* **8**, 2181 (1995).

17. S. Tett, *ibid.*, p. 1473.

18. G. A. Meehl and W. M. Washington [*Nature* **382**, 56 (1996)] provide an alternative mechanism for greater east Pacific warming. Following V. Ramanathan and W. D. Collins [*ibid.* **351**, 27 (1991)], they assumed that the albedo of deep convective clouds increases with SST. As the climate warms, this larger albedo reduces the solar radiation absorbed in the west Pacific relative to that in the east. This cirrus cloud thermostat mechanism has been criticized by some [see, for example, R. Fu, A. D. DelGenio, W. B. Rossow, W. T. Liu, *ibid.* **358**, 394 (1992); D. Hartmann and M. Michelson, *J. Clim.* **6**, 2049 (1993); R. T. Pierrehumbert, *J. Atmos. Sci.* **52**, 1784 (1995)].

19. "Coupling" is used in the ENSO literature to mean a feedback loop wherein a given change in SST causes a change in equatorial wind stress that results in a change in thermocline depth and finally SST. The ratio of the final to initial SST change would be a measure of "coupling" strength. Note that the oceanic changes are dynamical. Thermodynamics enters the loop only through its effect on wind stress.

20. N. C. Lau, S. G. H. Philander, M. J. Nath, *J. Clim.* **5**, 284 (1992); S. Manabe and R. J. Stouffer, *ibid.* **9**, 376 (1996); J. D. Neelin *et al.*, *Clim. Dyn.* **7**, 73 (1992).

21. A. Kaplan *et al.* (in preparation) present a global analysis and validation. The method [developed by A. Kaplan, M. A. Cane, Y. Kushnir, and B. Blumenthal (in preparation)] uses empirically derived time and space covariance estimates to obtain an optimally smoothed analysis of Atlantic SSTs from 1856 to 1991. The analysis procedure is similar to so-called "optimal interpolation" in that it uses estimates of spatial covariance to fill gaps in the data. In addition, it makes limited use of temporal covariance estimates in a Kalman Smoother algorithm; the SST data comes from (27).

22. Although the analysis extends from 1856 to 1991, we went back no further than 1900 because of suspicions that the 19th-century SSTs are systematically in error (1, 20).

23. The Lamont model has a well-known bias that places the maximum SST anomaly too far east; allowing for this would further increase the resemblance of Fig. 1 to the observed pattern.

24. K. Trenberth and T. Hoar, *Geophys. Res. Lett.* **23**, 57 (1996).

25. B. Rajagopalan, U. Lall, M. A. Cane, in preparation.

26. The global pattern correlation between Fig. 3, A and B, is 0.97. We also computed the first empirical orthogonal function of the data with ENSO removed; its principal component is largely trend and correlates with the trend patterns at 0.95 or more.

27. M. Bottomley, C. K. Folland, J. Hsiung, R. E. Newell, D. E. Parker, *Global Ocean Surface Temperature Atlas (GOSTA)* (Her Majesty's Stationary Office, London, 1990). This atlas is based on the U.K. Meteorological Office Main Marine Data Bank and includes corrections for systematic measurement errors. The version of the GOSTA data set that was used in (21), MOHSST5 [D. E. Parker *et al.*, in *Natural Climate Variability on Decade to*

Century Timescales (National Academy Press, Washington, DC, 1996), pp. 244–250], incorporates COADS (28) values where GOSTA data are deficient and uses an improved scheme of corrections for instrumental biases [C. K. Folland and D. E. Parker, *Q. J. R. Meteorol. Soc.* **121**, 319 (1995)].

28. S. D. Woodruff, R. J. Slutz, R. L. Jenue, P. N. Steurer, *Bull. Am. Meteorol. Soc.* **68**, 521 (1987).

29. Trends and confidence limits are based on a median estimator, the Sens slope test [see, for example, R. O. Gilbert, *Statistical Methods for Environmental Pollution Monitoring* (Van Nostrand Reinhold, New York, 1987)]. The more commonly used least squares trend estimates are less robust. The least squares trend estimates are (in degrees Celsius per century, with 95% confidence limits) $+0.72 \pm 0.63$ for the analysis, $+0.22 \pm 0.69$ for GOSTA, and $+0.35 \pm 0.62$ for COADS.

30. For a recent review with many references, see N. C. Lau, *Bull. Am. Meteorol. Soc.*, in press.

31. E. K. Schneider, B. Kirtman, R. S. Lindzen, *J. Clim.*, in press.

4 October 1996; accepted 27 December 1996

Potential Involvement of Fas and Its Ligand in the Pathogenesis of Hashimoto's Thyroiditis

Carla Giordano,* Giorgio Stassi,* Ruggero De Maria,*
Matilde Todaro, Pierina Richiusa, Giuliana Papoff,
Giovina Ruberti, Marcello Bagnasco, Roberto Testi,†
Aldo Galluzzo

The mechanisms responsible for thyrocyte destruction in Hashimoto's thyroiditis (HT) are poorly understood. Thyrocytes from HT glands, but not from nonautoimmune thyroids, expressed Fas. Interleukin-1 β (IL-1 β), abundantly produced in HT glands, induced Fas expression in normal thyrocytes, and cross-linking of Fas resulted in massive thyrocyte apoptosis. The ligand for Fas (FasL) was shown to be constitutively expressed both in normal and HT thyrocytes and was able to kill Fas-sensitive targets. Exposure to IL-1 β induced thyrocyte apoptosis, which was prevented by antibodies that block Fas, suggesting that IL-1 β -induced Fas expression serves as a limiting factor for thyrocyte destruction. Thus, Fas-FasL interactions among HT thyrocytes may contribute to clinical hypothyroidism.

The interaction of Fas (CD95/APO-1) with its ligand (FasL) regulates a number of physiological and pathological processes of cell death. Triggering of Fas contributes to the regulation of the immune response and tissue homeostasis, as well as to the immunological clearance of virus or tumor cells (1).

Hashimoto's thyroiditis (HT) is an autoimmune disorder in which destructive processes overcome the potential capacity of thy-

roid replacement, estimated as about 5- to 10-fold in a lifetime (2). Apoptosis has been occasionally observed in histological section of normal thyroid (3). However, apoptotic cell death is abnormally accelerated during the pathologic phases leading to clinical hypothyroidism (4).

The mechanisms responsible for thyrocyte destruction remain elusive (5). Normal thyrocytes do not express Fas (6). However, Fas is inducible in some cell types upon appropriate stimulation (1). To determine the possible involvement of Fas and its ligand in autoimmune thyroid destruction, we first analyzed Fas expression in thyroid specimens from active HT and from nontoxic goiter (NTG) patients. Immunohistochemistry of frozen thyroid sections and two-color flow cytometric analysis of dispersed thyroid follicular cells, obtained by enzymatic digestion, revealed that HT thyrocytes, identified for cytokeratin (Fig. 1A) and thyroperoxi-

C. Giordano, G. Stassi, M. Todaro, P. Richiusa, A. Galluzzo, Laboratory of Immunology, Endocrinology Section, Institute of Clinica Medica, University of Palermo, Palermo, Italy.

R. De Maria and R. Testi, Department of Experimental Medicine and Biochemical Sciences, University of Rome "Tor Vergata," Rome, Italy.

G. Papoff and G. Ruberti, Department of Immunobiology, Institute of Cell Biology, CNR, Rome, Italy.

M. Bagnasco, Allergy and Clinical Immunology, University of Genova, Genova, Italy.

*These authors contributed equally to this work.

†To whom correspondence should be addressed. E-mail: tesrob@flashnet.it